






Estimating an Indirect Solar Water Heater's Performance under the Latent Heat of Ethanol Using a Thermosiphon-Riser Collector

Hussein A. Mahmood^{*}, Ali D. Salman[†], Mohammed F. Mohammed[‡]

Department of Mechanical Engineering, University of Technology, Baghdad 000964, Iraq

Corresponding Author Email: me.20.10@grad.uotechnology.edu.iq

Copyright: ©2024 The authors. This article is published by IETA and is licensed under the CC BY 4.0 license (<http://creativecommons.org/licenses/by/4.0/>).

<https://doi.org/10.18280/ijht.420220>

ABSTRACT

Received: 10 January 2024

Revised: 15 March 2024

Accepted: 28 March 2024

Available online: 30 April 2024

Keywords:

filling ratio, ethanol, thermosiphon, water heater, thermal performance enhancers

The present work is investigated Describes a non-conventional solar water heater that uses a thermosiphon-riser collector and the domain latent heat for the intermediate working fluid (ethanol). Testing was done for the experimental investigation from 8 a.m. to 4 p.m. utilizing a test rig that was placed in Baghdad City and tilted 45 degrees to the south. The test apparatus is made out of a solar absorber matte paint. with dimensions of (80*120) cm and 0.5 mm thickness. 4 mm for a double acrylic cover. Filling ratios of 50% and 100% are used to evaluate the ethanol at flow rates of 1 and 1.5 L/min. on September 6, 8, 11, 13, and October 4, 5, 14, 16, 2022, in sunny days. These experiments were carried out in order to determine the ideal filling ratios, flow rates, and mechanisms for enhancing thermal performance. This process is accomplished by contrasting the thermosiphon-riser collector with and without the attached helical spring around the core bar. in closed loop system. The experimental results showed that the highest daily efficiency is (70%), according to the data, was achieved at 1.5 L/min flow rate with 50% filling ratio in case of helical spring around the core bar within the thermosiphon riser collector.

1. INTRODUCTION

The idea behind solar systems is to use the sun's heat to power a significant energy-related transportation system [1]. The concept was established by numerous academics and researchers, and it has since been applied widely in other fields. In addition to being less expensive to operate for lighting and warmth [2], solar systems are seen as environmentally beneficial a result to reduce the emissions of greenhouse gases because the fossil fuel usage be reduced [3]. This study will concentrate on the concept of using solar thermal energy to heat water, where it came from, and what improvements were made numerically, experimentally, and collaboratively. The most economical heating equipment is a thermosiphon solar water heating system, which requires no pumping energy [4]. Heat is transmitted in a thermosiphon tube by the processes of working fluid evaporation and condensation at the tube's top (condenser portion) and lower (evaporator section), respectively [5]. Samanci and Berber [6] and Kalogirou [7] examined the advantages of economics, environmental preservation, and thermal performance for four-person solar heating systems. The findings indicate that the annual value of the solar input was 79%. In addition, installing solar panels lowers greenhouse gas emissions and saves about 70% on petrol or electricity costs. Mathioulakis and Belessiotis [8] revealed investigation into a new kind of two-phase closed-loop thermosiphon solar heat collector that transfers heat directly from the collection to the water tank via an ethanol-filled heat pipe. The condensation section was poured into the water tank. The maximum instantaneous

efficiency of the system was 60%. Islam et al. [9] water, ethanol, and acetone were employed as working fluids to evaluate the performance of a water heating system's two-phase solar collector. To conduct experimental observations, they determined the collector's starting efficiency and adjusted the working fluid. discovered that productivity rose when ethanol was used in place of water or acetone. Samanci and Berber [6] have out an experimental comparison of two-phase (R-134a) closed thermosiphon water heating systems and single-phase (water) systems. Every experiment was conducted with the same load and conditions. demonstrated found the efficiency of 42.8% more was used in a two-phase system than in a single-phase system. The research of Balaji et al. [1] was done on the effect of a convection flat plate solar water heater with and without a thermal performance enhancer. Rod and tube are the two types of thermal performance enhancers that have been employed. The water flow rate of the Flat Plate Solar Water Heater ranged from 0.008 kg/s to 0.025 kg/s. the thermal performance enhancer achieved a maximum thermal efficiency of 74% at a flow rate of 90 kg/h. Aljuboori et al. [10] employed 185 W of constant heat input, three filling ratios (50, 70, and 90%), and a constant flow rate (2 l/m) for the condenser cooling water as the working fluid in order to verify by experimentation how the form of the evaporator affects the loop thermosiphon's heat transfer coefficient. In light of the experiment's findings, three distinct kinds of evaporator pipes. Three types of helical coil evaporators are used: I, which is straight; II, which has two turns and a coil diameter of 100 mm; and III, which has four turns and a coil diameter of 50 mm. Because it has a higher

heat transfer coefficient than types I and II, evaporator III performs better than the other two. It also has the highest effective thermal conductivity and the largest decrease in thermal resistance. Birajdar and Sewatkar [11] have examined how different adiabatic durations, filling ratios, and heat loads affect a closed-loop thermosyphon system when exposed to water, ethanol, acetone, and methanol. In comparison to the plate-type forced air-cooled condenser, it was found that the most efficient and with the lowest values (reducing overall thermal resistance by up to 72%) was the acetone-charged loop thermosyphon. The acetone-filled thermosyphon's adiabatic length was reduced to 200 mm from 800 mm, a 15% reduction in order to enhance performance. The loop thermosyphon with a water-cooled condenser was suggested to be replaced with a practicable plate-type forced air-cooled condenser due to its difficulties in cooling electronic components, computing clusters, and data centers. Koffi et al. [4] offered a thermosiphon-based evaluation of the thermal efficiency of a prototype solar heater with rolled copper tubes for internal exchange that crossed a sizable fluid mass with a diagonal hot water storage tank. The final result displayed the collected temperatures, mass flow rate, heat flux rate levels, and collector efficiency. These display a heat flux peak of 989 W/m², an outlet temperature of over 85.5°C, and a thermal efficiency of almost 58%. Taherian et al. [12] examined the dynamic modeling of a solar heating collector located in a horizontal storage tank. It was advised that the temperature of the fluid entering be as near to ambient as possible for the efficiency diagrams, useable energy, and temperatures of the inlet, exit, center of the glass cover, and center of the absorber. As a result, the findings revealed a mean efficiency of 68%, which falls as the ratio of temperature to incident radiation rises. Zelzouli et al. [13] examined the impact both theoretically and experimentally, of various inlet water temperatures on the collector's performance. The system is a high-performance thermosyphon that has low wall conductivity horizon storage and a glassed collector with a selective black coated absorber. Even with rising inlet water temperatures, the collector may still achieve high efficiency and high exit water temperature. according to experimental data. Based on numerical data, the DIFFEQ technical solution is able to anticipate the system's actual performance. With an experimental efficiency of 47.8% and a theoretical efficiency of 50%, polyurethane proved to be an excellent material for insulating thermal systems. Vijayan et al. [14] provided an overview of the research done on the flat plate solar collector system's performance. Both theoretical and actual tests and determined the variables influencing flat collector performance. They came to the conclusion that heating pipes, absorber plates, top coverings, and glazing all had a big impact on plate solar. Furthermore, the temperature outside, the tube's flow, solar insulation, maximum loss, the glass cover and plate's emissivity, slope, and coefficient all affect plate temperature, which in turn affects the collector's efficiency.

This design employs ethanol as a thermosiphon's working fluid setup to store steam. The purpose of this experiment was to employment indirect solar water heater based on the latent heat domain for the intermediate working fluid (ethanol) to investigate the optimum flow rate (1.5 and 1.5) L/min, filling ratios (50% and 100%), and the process to enhance the thermosiphon-riser collector's thermal performance by contrasting its use with and without the attached helical spring around the core bar.

2. EXPERIMENTAL SETUP

Figure 1 gives a detailed schematic architecture by using alcohol in the indirect solar water heater thermosiphon-collector raiser. Table 1 shows all dimensions of the experimental test rig. A matte-painted solar absorber copper sheet with dimension (80 by 120 cm) and (0.5 mm) thickness and two acrylic covers with (4 mm) thickness make up the flat plate solar collector, which is situated in Baghdad City and is tilted 45 degrees southward, is operational from 8 am to 4 pm. In addition, it has eight parallel copper riser pipes of 120 cm in length and 10.5 mm and 11.5 mm in inner and outer diameter, respectively. Ten centimeters separate the centerlines of adjacent tubes, and two headers at each end connect them. The upper header's diameter (41 mm) and length (80 cm) are made of copper. The copper used to make the lower header is 10.5 mm in diameter and 80 cm in length. Two apertures on the sides of the upper header are provided: one for the pressure gauge, and the other for the charging tube. The charging tube has an outside diameter of 6.35 mm and is used to create a vacuum, while the capillary tube has an outside diameter of 1 mm and is used to charge the working fluid. One opening vacuum tube with a 6.35 mm outer diameter is located in the lower header and is used to discharge the charge. Adapter screws are used to link the top riser headers, whereas welding is used to attach the lower headers. The main purpose of these adapter screws is to make it easier to remove riser pipes from headers in order to insert modification devices inside the riser pipes. To improve heat transfer, copper helical springs are positioned around an copper solid shaft inside riser pipes. The helical spring in this model creates a helical surface roughness by completely encircling the solid shaft and making contact with the riser pipes' interior surface. The solid shaft has a diameter of 6 mm and is welded shut on both sides, as seen in Figure 1(b). (13) A Mega 256 Arduino with thermocouples A K-type thermometer is used to measure the center and ends of the absorbent plate, the evaporator and condenser, the water entrance and exit, and the clear cover. The solar meter measures the incident solar power radiation on the collector between 0 and 2000 W/m². The system moves water by a small circulation pump (DC 24v), which has a maximum head of 3 m and a maximum flow rate from 1 to 3 L/min. For this experiment, flow rates of 1 and 1.5 L/min were selected. The flow rate in the test rig is regulated by a motor controller (PWM DC) motor speed regulator module (9V- 60V) is ideal speed controller, and a flow meter measures it. Before we went into the field, we made sure that every measurement device we utilized for this study was accurate by checking and adjusting it.

The water flow rate was calculated using the equation [15].

$$\dot{m}_w = \rho_w \cdot \dot{V}_w \quad (1)$$

This formula can be used to determine the useable energy across a collection in 30 minutes.

$$Q_u = \dot{m}_w \cdot C_w \cdot (T_{out} - T_{in}) \quad (2)$$

The daily solar radiation (G_{Td}) and daily energy utilization (Q_{ud}) were calculated with the trapezoidal rule [16].

$$Q_{ud} = b \left[\frac{Q_{u1}}{2} + Q_{u2} + Q_{u3} + \dots + \frac{Q_{un}}{2} \right] \quad (3)$$

B = time intervals = 1,800 seconds:

$$G_{Td} = A_c \cdot b \left[\frac{G_{T1}}{2} + G_{T2} + G_{T3} + \dots + \frac{G_{Tn}}{2} \right] \quad (4)$$

The daily efficiency can be calculated:

$$\eta_d = \frac{Q_{ud}}{G_{Td}} \quad (5)$$

To calculate the instantaneous efficiency [17]:

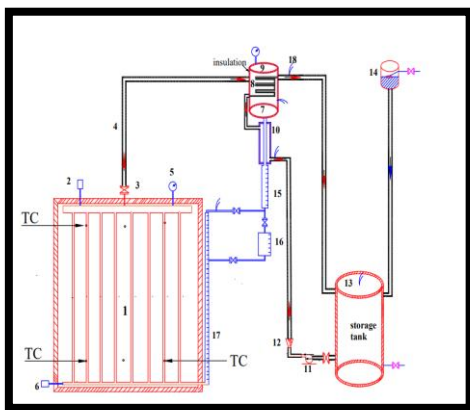
$$\eta_i = \frac{Q_u}{A_c \cdot G_T} \quad (6)$$



(a) The photo of the indirect solar water heating collector including a thermosiphon



(b) Helical spring inserted inside thermosiphon riser collectors



(c) The Schematic diagram of indirect solar water heating with a thermosiphon

Figure 1. Ethanol thermosiphon-riser collect system integrated with solar water heater

Table 1. All dimensions of the thermosiphon riser collector

No.	Parameters	Specification
1	Tubs	$D_o=10.5$ mm
	Upper header	$D_o=41$ mm
	Lower header	$D_o=6.35$ mm
2	Charge	$D_o=6.35$ mm
3	Valve	$D_o=6.35$ mm boll valve
4	Flexible tube	$D_i=8$ mm
5	Gauge pressure	2 bars
6	Discharge pipe	$D_o=6.35$ mm
7	Sub cool heat exchange pipe installed	$D_o = 7.9$ mm
8	Heat exchange	$D_o=6.35$ mm, $L=2$ m
9	Steam tank	$D_i=20$ cm, $L=30$ cm
10	Sub cool heat exchange	$D_o=25$ mm, $L=200$ mm
11	Water pump	200 L/h
12	Flow meter water	25-250 l/h
13	Storage tank hot water	40 L
14	Feed tank water	25 L
15	Cylinder with a graduated transparency	$D_i=5$ cm, $h=25$ cm
16	Transparent graduated tank	600 cc
17	Transparent graduated tube for level of working fluid	$D_o=12.7$ mm
18	Thermocouples	$^{\circ}C$

3 RESULTS AND DISCUSSION

3.1 Effect of filling ratio on useful energy

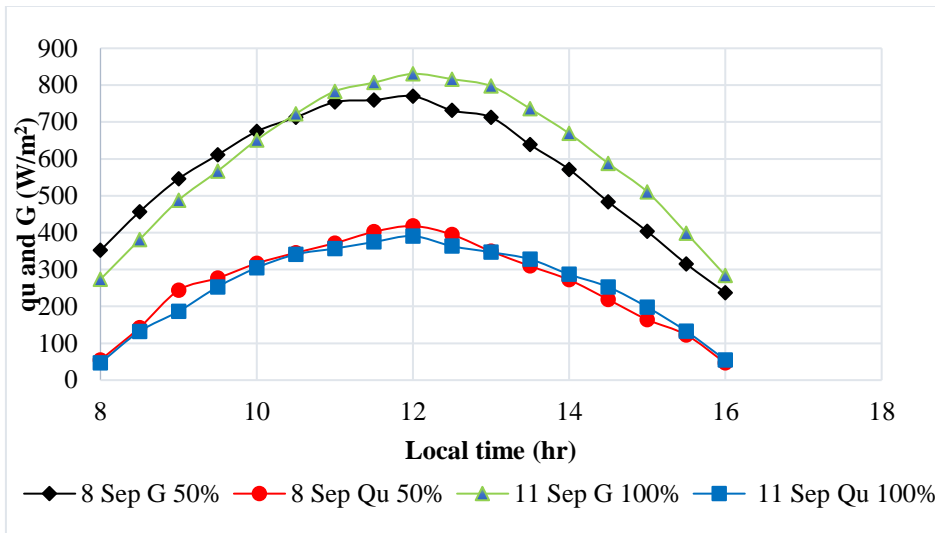
Figure 2 and Figure 3 present the energy produced increases starting at 8:30 and reaches its peak at noon. The energy used then steadily declines in proportion to solar radiation, reaching its minimum at 4:00 pm. The usable energy increases as the flow rate rises. Moreover, the usable energy rises as the filling ratio falls. Because there is less thermal resistance, the quantity of steam produced has increased., which ultimately results in a rise in the heat acquired quantity. Additionally, the impact of adding a helical springaround a core bare to thermosiphon risers in order to boost the usable energy for various filling ratios and flow rates in test rig system

3.2 Tank's temperature

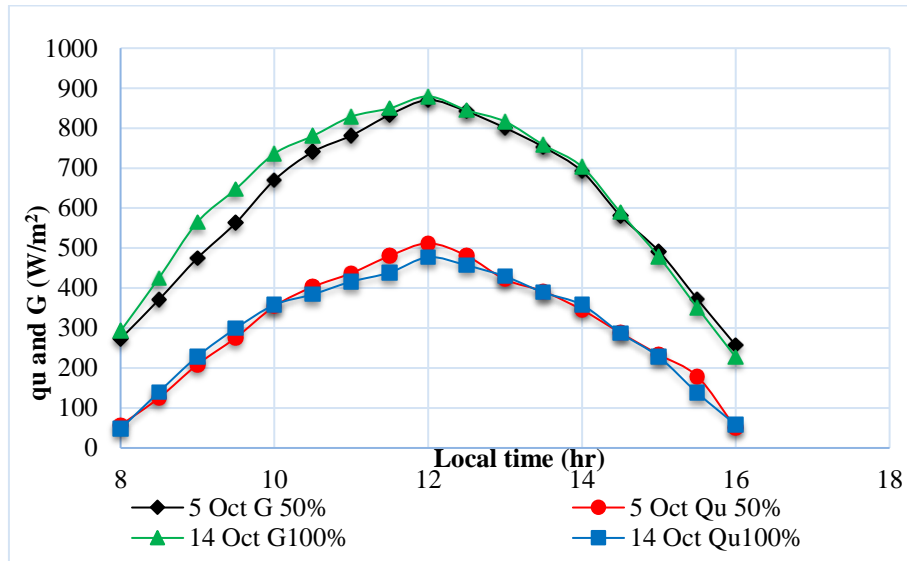
Figure 4 and Figure 5 show the comparison between solar radiation, storage tank temperature, and ambient temperatures at (50% and 100%) filling ratio, with and without inserted a helical spring around the core bar inside the thermosiphon riser collector, and varying flow rates. In case without inserted one, the temperature of the storage tank rose from 29.5 $^{\circ}C$ to 65.5 $^{\circ}C$ and, in the absence of an inserted filter, from 28.8 $^{\circ}C$ to 68.8 $^{\circ}C$ when the filling ratio was 50% at flow rates of 1 and 1.5 L/min, respectively. However, the temperature of the storage tank rises by 18% and 14%, respectively, when a helical spring is inserted at a flow rate of 1, 1.5 L/min. When filling ratio is increased to 100% With flow rates of 1, 1.5 L/min, The storage tank's temperature increased from 28.8 $^{\circ}C$ to 60.4 $^{\circ}C$ and from 28.8 $^{\circ}C$ to 60.4 $^{\circ}C$, respectively, When the helical spring around the core bar is inserted the thermosiphon's rise, the percentage in storage tank temperature is 18% and 15%, respectively, at flow rates of 1

and 1.5 L/min. this effect results from the storage tank's temperatures remaining elevated until 3:30 PM even after midday when sun radiation starts to decline. This behavior is caused by the heat-storing action of the collector plate's heat capacity as well as the vapor working liquid inside the

thermosyphon. The temperature storage tank naturally decreases after 3:30 PM. The drop in solar radiation at sunset and the surrounding temperature are the cause of this behavior, which increases the thermal energy that is lost from the storage tank.

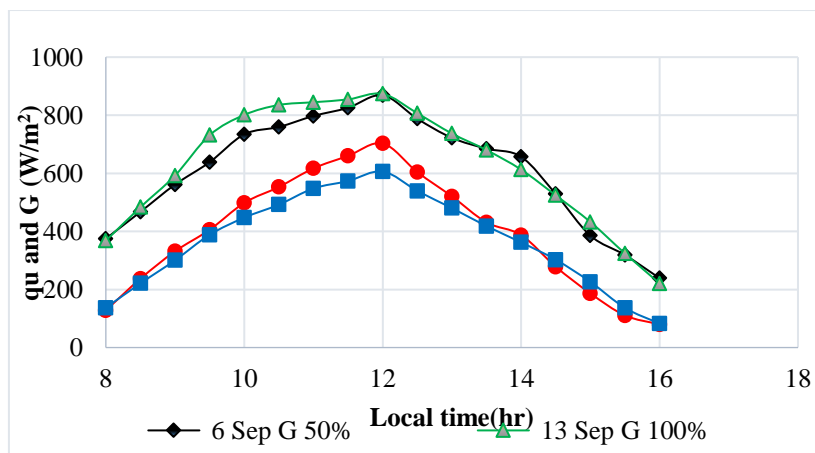


(a) (1) L/min flow rate and (50%, 100%) filling ratio without an enhancement device

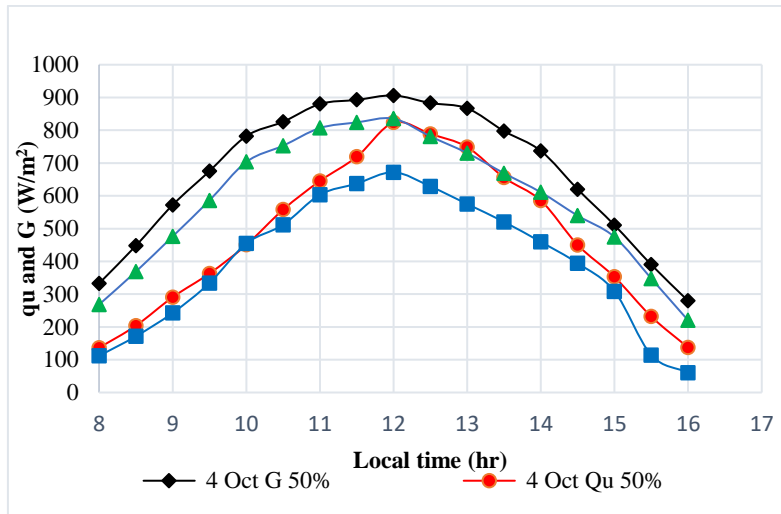


(b) (1) L/min flow rate and (50%, 100%) filling ratio with an enhancement device

Figure 2. comparison the solar radiation and useful energy at (1) L/min a flow rate and (50%, 100%) filling ratio with and without the enhancement device

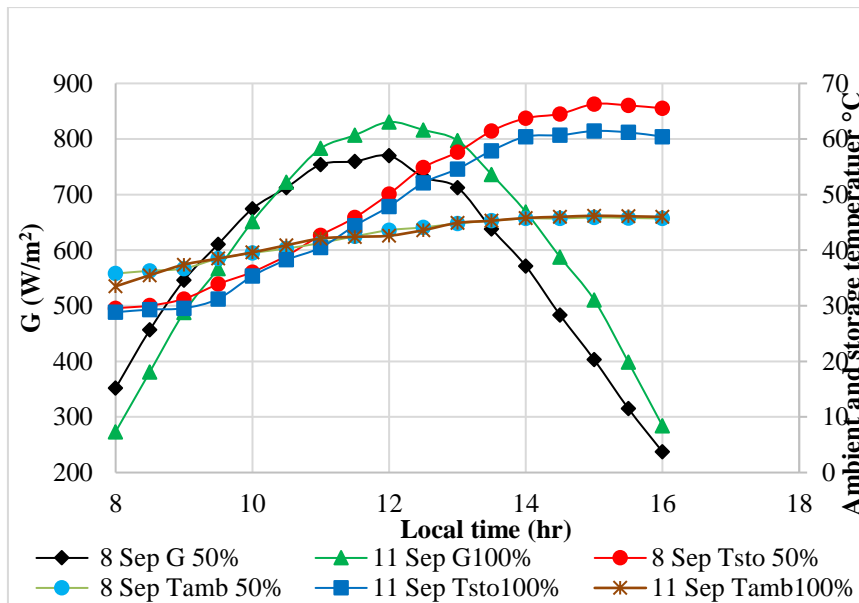


(a) (1.5) L/min flow rate and (50%, 100%) filling ratio without an enhancement device

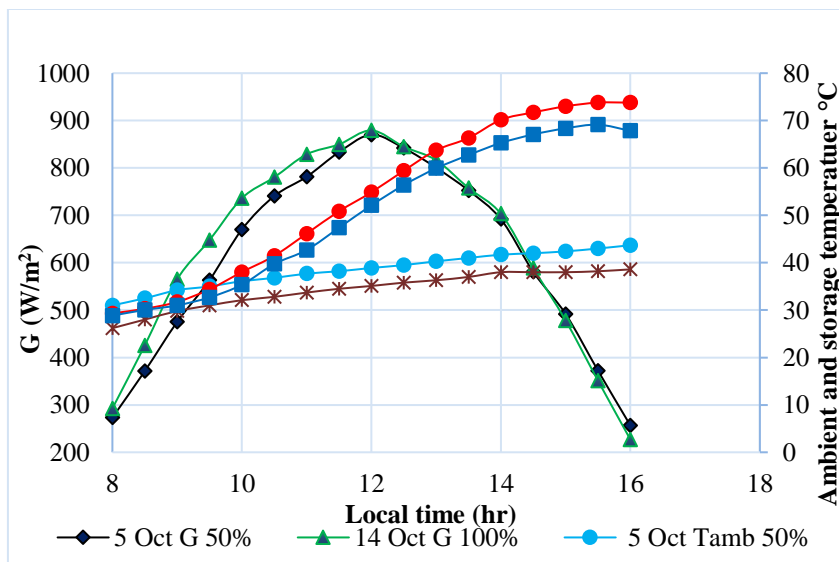


(b) (1.5) L/min flow rate and (50%, 100%) filling ratio with an enhancement device

Figure 3. comparison the solar radiation and useful energy for (1) L/min a flow rate and (50%, 100%) filling ratio with and without the enhancement device

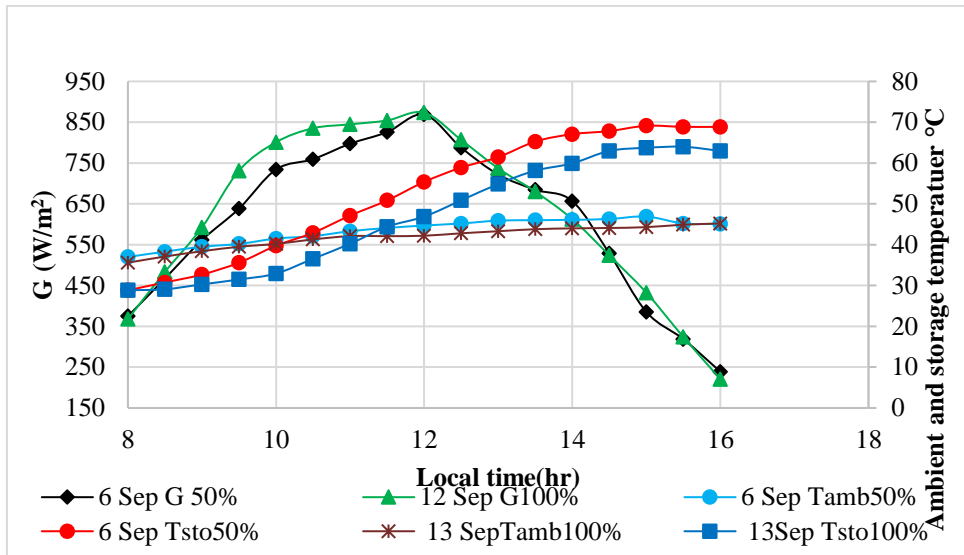


(a) L/min flow rate and (50%, 100%) filling ratio without an enhancement device

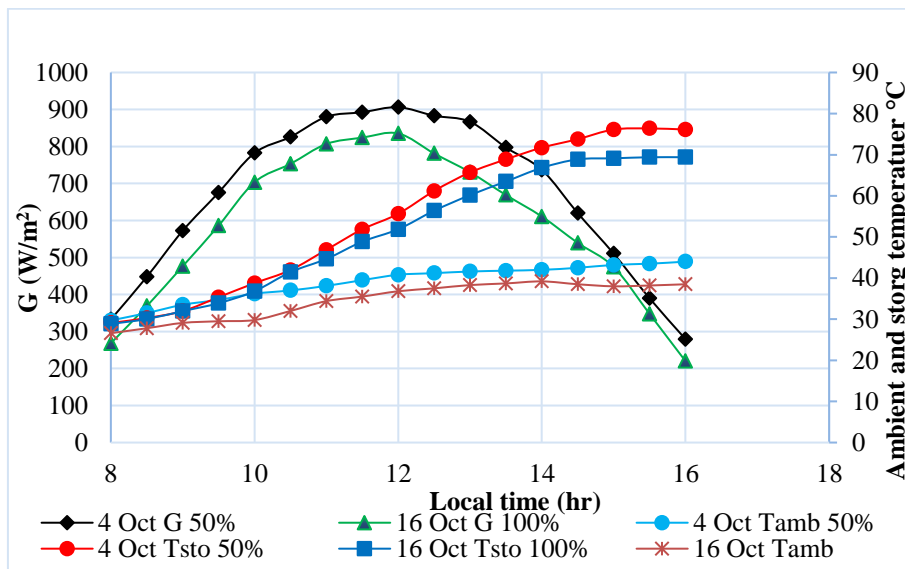


(b) L/min flow rate and (50%, 100%) filling ratio with an enhancement device

Figure 4. Comparison the solar radiation, ambient and storage temperature for L/min a flow rate and (50%, 100%) filling ratio with and without the enhancement device



(a) (1.5) L/min flow rate and (50%, 100%) filling ratio without an enhancement device



(b) L/min flow rate and (50%, 100%) filling ratio with an enhancement device

Figure 5. comparison the solar radiation, ambient and storage temperature for L/min a flow rate and (50%, 100%) filling ratio with and without the enhancement device

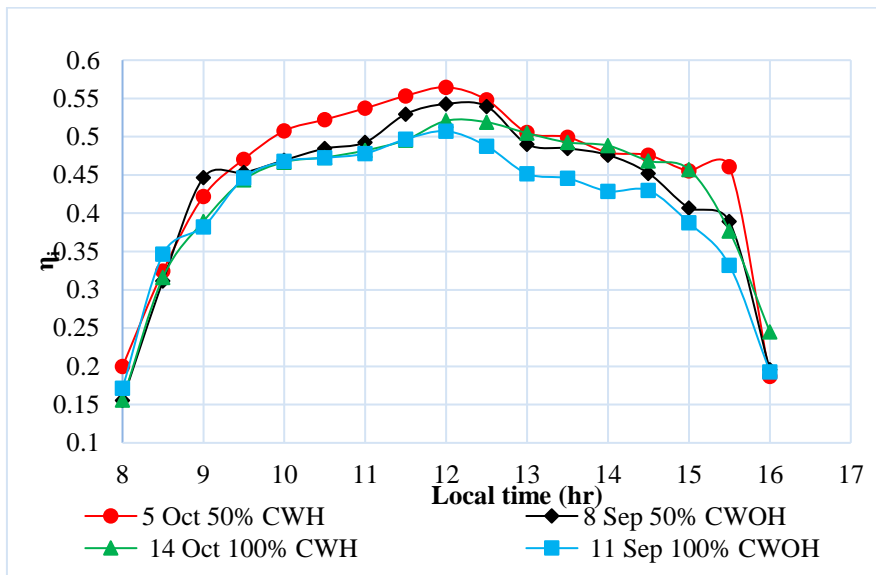


Figure 6. Comparison the efficiency for L/min a flow rate and (50%, 100%) filling ratio with and without the enhancement device

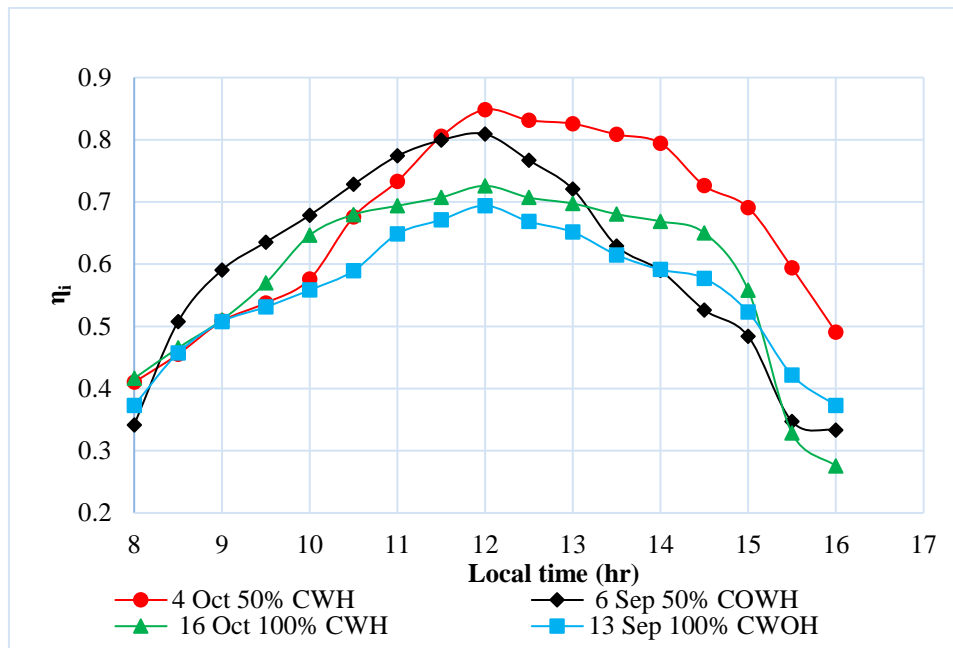


Figure 7. comparison the efficiency for (1.5) L/min a flow rate and (50%, 100%) filling ratio with and without the enhancement device

3.3 Efficiency

Figure 6 and Figure 7, on a sunny day, plot efficiency in relation to flow rate and filling ratio. These graphs show that as flow rate increases, less heat is lost to the surrounding air. This is because increasing the flow rate causes the absorbing plate to absorb more energy, which lowers the temperature differential between the ambient and collector absorber and ultimately boosts daily efficiency. Apart from wind speed, how many coverings are there, and what sort of insulators are employed, Thermal losses are influenced by a number of variables, including the amount of solar energy received and the weather conditions. The data shows that when a helical spring around the core bare is placed, the maximum daily efficiency is 70% at filling ratio is 50% and the flow rate is 1.5 L/min.

4. CONCLUSION

The following conclusions can be drawn based on this study:

- The alcohol thermosiphon-riser collector indirect solar water heater was the subject of an experimental investigation with varying filling ratios and flow rates. Thermosiphon riser solar collector's highest daily efficiency was 70%, up from a declining ratio of 50% while using an enhancement device (1.5 L/min).
- At flow rate (1.5 L/min) and the filling ratio (50%), the daily efficiency increases by 7% when used with an enhancement device as opposed to not using.
- At flow rate (1.5 L/min) and the filling ratio (50%), the daily efficiency increases by (14%) when used with an enhancement device as opposed filling ratio (100%) with enhancement at flow rate (1.5 L/min).
- The storage tank's temperature increased by (14%) when the enhancement device was used in conjunction with a 50% filling ratio rather than

without it.

- When working with a filling ratio of 50% with an enhancement device rather than 100% with enhancement at the temperature of the storage tank increased. by 16%. at a flow rate of 1.5 L/min.
- In summary, because it possesses the necessary thermal performance, Use of this collector in solar water heating systems is ideal.
- The heat transfer coefficient of change-phase solar water heating systems is much higher than that of single-phase convective heat transfer when boiling and condensing are included, making them superior to single-phase solar water heaters.
- The thermal performance of thermosiphon risers is improved when ethanol alcohol is used as the working fluid since it has a lower boiling point than water, which increases the rate of heat transfer.

The following are recommended for the future research in this field:

- Simulating the current work with TRANSYS software.
- Employing blends as a working fluid.
- Researching how natural condenser design geometries affect the solutions increases the capacity for heat transmission from the condenser to the evaporator, potentially reducing the thermal resistance of the condenser.

REFERENCES

- [1] Balajia, K., Idrish Khanb, A., Ganesh Kumarc, P., Iniyana, S., Goicd, R. (2019). Experimental analysis on free convection effect using two different thermal performance enhancers in absorber tube of a forced circulation flat plate solar water heater. *Solar Energy*, 185: 445-454.

- <https://doi.org/10.1016/j.solener.2019.04.089>
- [2] Aung, N.Z., Li, S. (2013). Numerical investigation on effect of riser diameter and inclination on system parameters in a two-phase closed loop thermosyphon solar water heater. *Energy Conversion and Management*, 75: 25-35. <https://doi.org/10.1016/j.enconman.2013.06.001>
- [3] Vengadesan, E., Senthil, R. (2020). A review on recent development of thermal performance enhancement methods of flat plate solar water heater. *Solar Energy*, 206: 935-961. <https://doi.org/10.1016/j.solener.2020.06.059>
- [4] Koffi, P.M.E., Andoh, H.Y., Gbaha, P., Touré, S., Ado, G. (2008). Theoretical and experimental study of solar water heater with internal exchanger using thermosiphon system. *Energy Conversion and Management*, 49(8): 2279-2290. <https://doi.org/10.1016/j.enconman.2008.01.032>
- [5] Nada, S.A., El-Ghetany, H.H., Hussein, H.M.S. (2004). Performance of a two-phase closed thermosyphon solar collector with a shell and tube heat exchanger. *Applied Thermal Engineering*, 24(13): 1959-1968. <https://doi.org/10.1016/j.applthermaleng.2003.12.015>
- [6] Samanci, A., Berber, A. (2011). Experimental investigation of single-phase and two phase closed thermosyphon solar water heater systems. *Scientific Research and Essays*, 6(4): 688-693.
- [7] Kalogirou, S. (2009). Thermal performance, economic and environmental life cycle analysis of thermosiphon solar water heaters solar energy. *Elsevier*, 83(1): 39-48. <https://doi.org/10.1016/j.solener.2008.06.005>
- [8] Mathioulakis, E., Belessiotis, V. (2002). A new heat-pipe type solar domestic hot water system. *Solar Energy*, 72(1): 13-20. [https://doi.org/10.1016/S0038-092X\(01\)00088-3](https://doi.org/10.1016/S0038-092X(01)00088-3)
- [9] Islam, M.A., Khan, M.A.R., Sarkar, M.A.R. (2005). Performance of a two-phase solar collector in water heating. *Journal of Energy & Environment*, 4: 117-123.
- [10] Aljuboori, A.A.A., Ahmed, S.Y., Jabbar, M.Y. (2020). Experimental study of closed loop thermosyphon with a different evaporator geometry. *Heat Transfer*, 50(1): 466-486. <https://doi.org/10.1002/htj.21887>
- [11] Birajdar, M.R., Sewatkar, C.M. (2021). Experimental investigation of the loop thermosyphon with different adiabatic lengths charged with different working fluids. *Heat Transfer*, 50(5): 4171-4191. <https://doi.org/10.1002/htj.22070>
- [12] Taherian, H., Rezaia, A., Sadeghi, S., Ganji, D.D. (2011). Experimental validation of dynamic simulation of the flat plate collector in a closed thermosyphon solar water heater. *Energy Conversion and Management*, 52(1): 301-307. <https://doi.org/10.1016/j.enconman.2010.06.063>
- [13] Zelzouli, K., Guizani, A., Kerkeni, C. (2014). Numerical and experimental investigation of thermosyphon solar water heater. *Energy Conversion and Management*, 78: 913-922. <https://doi.org/10.1016/j.enconman.2013.08.064>
- [14] Vijayan, S.N., Karthik, S., Vijayaraj, V.T. (2016). Assorted performance investigation of flat plate solar collector - A review. In *International Conference on Systems, Science, Control, Communication, Engineering and Technology*.
- [15] Duffie, J.A., Beackman, W.A.B. (2013). *Solar Energy of Thermal Processes*. John Wiley and Sons. <https://doi.org/10.1002/9781118671603>
- [16] Scheid, F. (1989). *Numerical Analysis*, Second edition. McGraw-Hill Book Company.
- [17] Rittidech, S., Donmaung, A., Kumsombut, K. (2009). Experimental study of the performance of a circular tube solar collector with closed-loop oscillating heat-pipe with check valve (CLOHP/CV). *Renewable Energy*, 34(10): 2234-2238. <https://doi.org/10.1016/j.renene.2009.03.021>

NOMENCLATURE

Symbols

A_C	Collector area, m^2
c_w	Water specific heat, $J/kg.K$
G_T	Total solar radiation, W/m^2
G_{Td}	Daily solar radiation, W/m^2
Q_{ud}	Daily useful energy, W
Q_u	Useful energy, W
\dot{m}_w	Water flow rate, kg/s
\dot{V}_w	Volume flow rate of water, m^3/s
T_{in}	Inlet water temperature, $^{\circ}C$
T_{out}	Outlet water temperature, $^{\circ}C$

Greek symbols

ρ_w	Density of water, kg/m^3
η_d	Daily efficiency
η_i	Instantaneous efficiency